Global Energy Interconnection
Development and Cooperation Organization

ELSEVIER
Production And Hosting By Elsevier On Behalf Of KeAi
KeAi

Volume 4 Number 3 June 2021 (251-260)
DOI: 10.14171/j.2096-5117.gei.2021.03.003
Global Energy Interconnection
Contents lists available at ScienceDirect
https: //www.sciencedirect.com/journal/global-energy-interconnection

Full-length article

Two-stage ADMM-based distributed optimal reactive power control method for wind farms considering wake effects

Zhenming Li[1,2], Zhao Xu[1], Yawen Xie[3], Donglian Qi[2], Jianliang Zhang[2]

1. Department of Electrical Engineering, The Hong Kong Polytechnic University, Kowloon, HKSAR, P.R. China
2. College of Electrical Electronic Engineering, Zhejiang University, Hangzhou, P.R. China
3. Quzhou Power Supply Company, Zhejiang Electric Power Company of State Grid, Quzhou, P.R. China

Scan for more details

Abstract: Since the connection of small-scale wind farms to distribution networks, power grid voltage stability has been reduced with increasing wind penetration in recent years, owing to the variable reactive power consumption of wind generators. In this study, a two-stage reactive power optimization method based on the alternating direction method of multipliers (ADMM) algorithm is proposed for achieving optimal reactive power dispatch in wind farm-integrated distribution systems. Unlike existing optimal reactive power control methods, the proposed method enables distributed reactive power flow optimization with a two-stage optimization structure. Furthermore, under the partition concept, the consensus protocol is not needed to solve the optimization problems. In this method, the influence of the wake effect of each wind turbine is also considered in the control design. Simulation results for a mid-voltage distribution system based on MATLAB verified the effectiveness of the proposed method.

Keywords: Two-stage optimization, Reactive power optimization, Grid-connected wind farms, Alternating direction method of multipliers (ADMM).

0 Introduction

There is a prevailing trend to integrate various renewable energy generation sources into modern power systems featuring sustainable development and decarbonization. Among all others, wind energy distinguishes itself with its advantages of considerable power capacity, high efficiency, and wide availability. Particularly, the doubly fed induction generator (DFIG) has attracted significant attention owing to its low cost and flexible controllability. Specifically, the active and reactive power of the DFIG can be decoupled and controlled independently, which facilitates its manipulation of reactive power generation and voltage support to the grid.

The use of voltage and reactive power control systems is mandated in modern wind farms (WFs). They are used to regulate the voltage at the point of connection (POC) within a certain range to counteract the destabilization effects of intermittent wind power generation. Meanwhile, the terminal voltage of wind turbines (WTs) must be maintained within a feasible range to prevent trips of WTs caused by severe faults [1]. As wind generation exhibits a strong

Received: November 10 2020 Accepted: May 11 2021 Published: June 25 2021

✉ Donglian Qi
qidl@zju.edu.cn

Yawen Xie
841219920@qq.com

Zhenming Li
lizm1994@zju.edu.cn

Jianliang Zhang
jlzhang@zju.edu.cn

Zhao Xu
zhao.xu@polyu.edu.hk

potential for grid voltage stabilization, several studies have reported that wind generation is a feasible dispatch resource to control and optimize the reactive grid power flow [2].

Centralized control algorithms such as secondary proportional integral (PI) control, model predictive control, and artificial intelligence algorithms have been applied for reactive power control of WFs and WTs. As reported in [3,4], the secondary PI control can be applied to operate the grid-tied WT reactive power for eliminating the grid voltage fluctuation. A direct voltage control method, which can keep the terminal voltage within an acceptable range, is proposed in [5] to protect the associated grid appliances. Based on the Adaptive Nondominated Sorting Algorithm III and the Latin Hypercube Sampling Algorithm, a robust dynamic reactive power optimization method is reported in [6] for the reactive power control of wind power generation. In [7], the particle swarm optimization (PSO) algorithm is used to find the optimal reactive power output of WFs to minimize the distribution loss. Reference [8] formulates an optimization problem to maximize the renewable energy harvesting within the operational and environmental limitations for a wind-photovoltaic hybrid renewable energy system. However, centralized control schemes have drawbacks such as (i) high communication cost, (ii) heavy computational load [9,10], (iii) slow computing speed, and (iv) stringent hardware requirements in large-scale WFs.

Among distributed optimization control methods [11-14], the ADMM algorithm, which is applied to solve large-scale convex optimization problems, has been reported to optimize the reactive power of the grid in a distributed manner [15]. Similar research has been reported in [16], where the coordination among reactive power sources of multiple WFs in a voltage-source-converter high-voltage DC system is achieved. To minimize the losses of the generators, converters, filters, and the grid, a distributed optimal reactive power control scheme based on ADMM is proposed in [17]. This optimization scheme only demands information exchange between adjacent controllers, which reduces the communication infrastructure. In addition, to achieve the optimal coordination among grid, WFs, and WTs subjected to multiple constraints and optimization objectives, a hierarchical optimization structure has also been reported [18-21]. By combining the two-layer optimization structure and the ADMM algorithm, the WF reactive power reference is optimized in the first layer optimization structure according to the dispatch command from the transmission system operators (TSO). Then, the reactive power outputs of WTs in the WF are optimized in the second layer [22-24].

In the practical ADMM algorithm application, the global variable change is usually taken as the convergence criterion. In recent studies, the utilization rate of WFs or WTs is considered as the global variable and the consensus of utilization ratio is modeled as the convergence criterion [17,22]. However, the consensus of utilization ratio is an ideal assumption. The idea of area partition is used to manage this problem. It can be considered as a centralized supportive distributed algorithm, which has been discussed in several articles [25-27]. In the partitioning algorithm, only the coupled region information is exchanged between adjacent regions. Compared with the aforementioned consensus-based ADMM algorithm, the partition-based ADMM algorithm is more flexible in global variable selection. The idea of partition has been reported in [26,27] to determine whether the algorithm will converge by comparing the change of state variables in the coupled region.

When considering the control and optimization algorithm design, wake effect is an important issue for large-scale WFs [28-32]. However, fewer studies have discussed voltage optimization considering the wake effect, which is one of our study's contributions.

Based on this philosophy, a two-stage distributed reactive power output optimization control method is proposed in this study. The key contributions can be summarized as follows:

i) A two-stage optimization structure is established. The upper layer is used to optimize the reactive power in the distribution network with the objective of tracking TSO reactive power dispatch commands. The lower layer is applied to optimize the reactive power among the WFs and track reactive power commands generated by the distribution network layer.

ii) Based on the idea of partition, the coordination of distributed reactive power flows is simultaneously optimized in both the grid and WF layers.

iii) In the WF layer, the wake effect is modeled with respect to different weighting factors, which is more consistent with the practical situation.

The remainder of this article is organized as follows. The proposed two-stage distributed voltage optimization control scheme is discussed in Section 1. Then, the loss calculation of the grid and WF is elaborated in Section 2. Details about ADMM and the proposed optimization method are presented in Section 3. Simulation verifications are provided in Section 4. Finally, the conclusions and potential future work are summarized in Section 5.

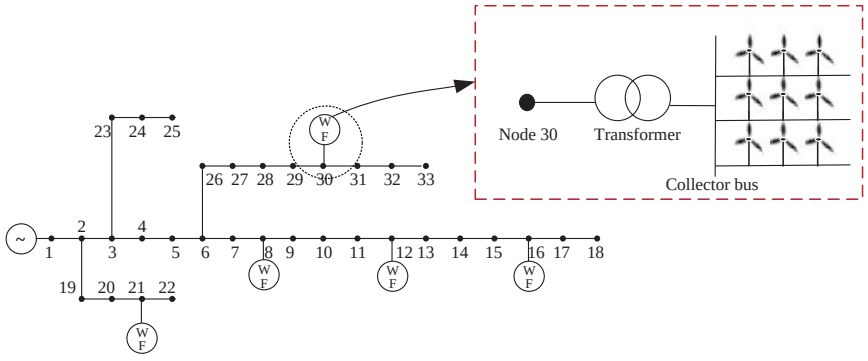

Fig. 1 Example of the WF structure connected to the distribution network

1 Modeling of the proposed two-stage distributed voltage optimization control scheme

1.1 Structure of the grid-connected WFs

Fig. 1 shows the typical WF structure connected to the distribution network through transformers. It is supposed that several WFs are connected to the distribution network through collector buses, and each collector bus is connected to several feeders, to which several WTs are connected.

1.2 Structure of the double-fed induction WT

Fig. 2 shows the structure of the double-fed induction WT when connected to a feeder. The WT blades are connected to the generator through a gearbox. The WT stator is directly connected with the feeder to realize the active and reactive power exchange with the feeder. Additionally, the WT rotor is connected to the feeder through a rotor-side converter (RSC) and a grid-side converter (GSC), where active power, reactive power, and frequency are controlled by AC excitation. With the electronic converters, the active and reactive power produced by WTs can be independently controlled.

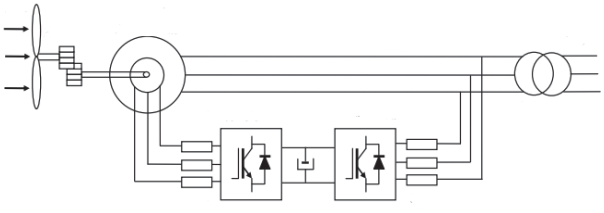

Fig. 2 Structure of the double-fed induction wind turbine [33]

1.3 Structure of distributed voltage optimization control

Fig. 3 shows an example of the proposed structure of the distributed voltage optimization control method. It is composed of two calculation stages:

First stage: Calculation of Q_{WFi}^{ref} in the distribution network layer. The reactive power reference Q_{WFi}^{ref} is decided for several areas of the distribution network, with an objective to minimize the total power losses in the distribution network. To solve the optimization problem in a distributed manner, the distribution network is separated into several areas, and each area is equipped with a controller to ensure that it can operate only with the local measurements and data from the neighboring area.

Second stage: Calculation of Q_{WTi}^{ref} in the WF layer. The reactive power reference Q_{WTi}^{ref} of each WT is decided by WT controllers according to the Q_{WFi}^{ref} received from the first layer. The WTs in the WF operate in a distributed manner to minimize the total power losses inside the WF. To make full use of the reactive power potential under the premise of considering the active power output, wake effects will be considered while tracking the Q_{WTi}^{ref} command.

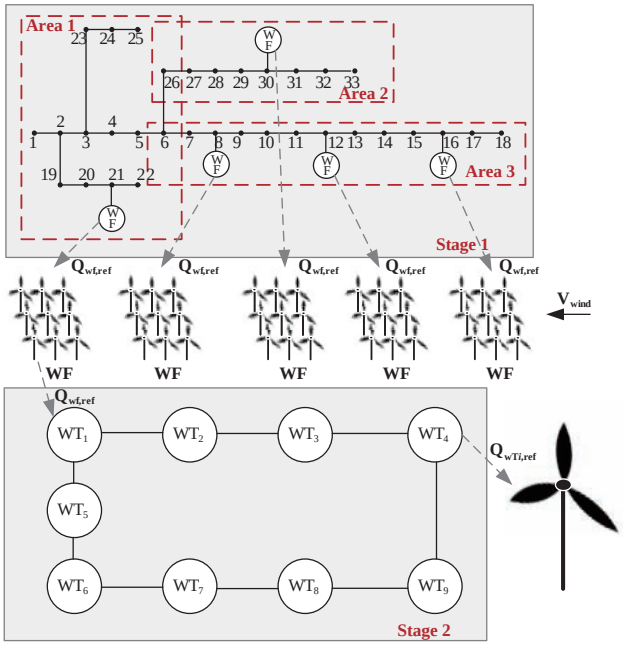

Fig. 3 Example of the proposed structure of the distributed voltage optimization control method

2 Loss calculation of the grid and the WF

Loss calculation is presented in this section, including the loss calculation of the distribution network and the WFs.

2.1 Loss calculation of the grid

As for the voltage optimization control of the distribution network, it is a primary condition that the voltage of each node in the system runs within the allowable range. Furthermore, economic operation is also an important factor to consider. In this study, active power loss is proposed as an indicator to reflect network loss:

$$P_{grid}^{loss} = \sum_{i=1}^{n-1}\sum_{j=i+1}^{n} I_{ij}^2 R_{ij} = \sum_{i=1}^{n-1}\sum_{j=i+1}^{n} \frac{P_{ij}^2 + Q_{ij}^2}{V_i^2} R_{ij} \tag{1}$$

where I_{ij} is the current on $Line_{ij}$, R_{ij} is the resistance of $Line_{ij}$, V_i is the voltage of $Node_i$, P_{ij} is the active power at the head of $Line_{ij}$, Q_{ij} is the reactive power at the head of $Line_{ij}$, and i, j is the node number of the distribution network with N nodes in total, $i, j \in \{1, 2, \cdots N\}$.

Based on Kirchhoff's law of voltage and current, we can obtain the power flow as follows:

$$P_{ij} = \sum P_{jk} - \frac{P_{ij}^2 + Q_{ij}^2}{V_i^2} R_{ij} - P_j^{load} + P_j^{WF} \tag{2}$$

$$Q_{ij} = \sum Q_{jk} - \frac{P_{ij}^2 + Q_{ij}^2}{V_i^2} X_{ij} - Q_j^{load} + Q_j^{WF} \tag{3}$$

$$V_j^2 = V_i^2 - 2(R_{ij}P_{ij} + X_{ij}Q_{ij}) + (R_{ij}^2 + X_{ij}^2)\frac{P_{ij}^2 + Q_{ij}^2}{V_i^2} \tag{4}$$

$$V_1 = V_N \tag{5}$$

where X_{ij} is the reactance of $Line_{ij}$; V_N is the rated voltage of the network (supposing that $Node_1$ is the generator node); $\sum P_{jk}$ and $\sum Q_{jk}$ are the sums of the active and reactive power from $Node_j$ to $Node_k$, respectively; P_j^{load} and Q_j^{load} are the active and reactive power of nodal nodes, respectively; Q_j^{WF} and Q_j^{WF} are the active and reactive power produced by $Node_j$, respectively, and are defined as

$$P_j^{WF},\ Q_j^{WF} \begin{cases} > 0, \ if\ Node_j\ connects\ to\ a\ WF \\ = 0, \ if\ Node_j\ is\ a\ load\ node \end{cases} \tag{6}$$

Furthermore, the reactive power that a WF can produce is limited by its capacity and active power, that is,

$$\left|Q_j^{WF}\right| \leqslant Q_j^{WF\ \max} = \sqrt{\left(S_j^{WF}\right)^2 - \left(P_j^{WF}\right)^2} \tag{7}$$

where $Q_j^{WT\ \max}$ is the maximum reactive power that a WF connects to $Node_j$ can produce, and S_j^{WT} is the apparent power of the WF.

According to the operational requirements of the distribution network, the voltage is supposed to satisfy,

$$0.95\ p.u. \leqslant V_j \leqslant 1.05\ p.u. \tag{8}$$

2.2 Loss calculation of the WF

Because the WF model is also a radial network [12], the WF connection mode can be determined by referring to the distribution network model. The WF loss is primarily composed of loss from collector bus to slack bus, feeder loss, and component loss of WTs. Reference [17] provides the calculation model of the loss of each part, which is referenced in this study.

The collector bus losses can be calculated as,

$$P_{col}^{loss} = R_{col}\frac{P_{col}^2 + Q_{col}^2}{V_{col}^2} \tag{9}$$

where R_{col} is the resistance between the collector and slack buses. P_{col} and Q_{col} are active and reactive power from the slack bus to the collector bus, respectively. V_{col} is the voltage of the collector bus.

The feeder loss is modeled as,

$$P_{fd}^{loss} = \sum_{i,j=1}^{n_{WT}} R_{i,j}\frac{P_{i,j}^2 + Q_{i,j}^2}{V_i^2} \tag{10}$$

where $R_{i,j}$ is the resistance between node i and node j, $P_{i,j}$ and $Q_{i,j}$ are active and reactive power from node i to node j, respectively. V_i is the voltage of node i.

The component loss of a WT is modeled as,

$$P_{WT}^{loss} = P_{cp}^{loss} + P_{conv}^{loss} + P_{fil}^{loss} \tag{11}$$

where P_{cp}^{loss} is defined as copper losses in the stator and rotor, P_{conv}^{loss} is the losses of converters (rotor- and grid-side converters), and P_{fil}^{loss} is the losses of the filters.

Based on the calculation models in [17], P_{cp}^{loss}, P_{conv}^{loss}, and P_{fil}^{loss} can be calculated as,

$$\begin{aligned} P_{WF}^{loss} &= \sum_{i=1}^{N_T} P_{WTi}^{loss} = \sum_{i=1}^{N_T} I^T R I \\ &= \sum_{i=1}^{N_T} (AQ_s + B)^T R (AQ_s + B) \end{aligned} \tag{12}$$

$$\begin{aligned} P_{conv}^{loss} &= P_{RSC}^{loss} + P_{GSC}^{loss} \\ &= P_{cr} + R_{cr}(I_{RSC}^{rms\ 2} - c_r^2) + P_{cg} + R_{cg}(I_{GSC}^{rms\ 2} - c_g^2) \\ &= C + R_{cr}(I_{dr}^2 + I_{qr}^2) + R_{cg}(s^2 I_{ds}^2 + \frac{Q_g^2}{V_s^2}) \\ &= HQ_s^2 + JQ_s + R_{cg}\frac{Q_g^2}{V_s^2} + K \end{aligned} \tag{13}$$

$$\begin{aligned} P_{fil}^{loss} &= R_{fil}(I_{dg}^2 + I_{qg}^2) \\ &= R_{fil}(s^2 I_{ds}^2 + \frac{Q_g^2}{V_s^2}) \\ &= R_{fil}(s^2(a_1^2 Q_s^2 + 2a_1 b_1 Q_s + b_1^2) + \frac{Q_g^2}{V_s^2}) \end{aligned} \tag{14}$$

where $R = diag(R_s, R_s, R_r, R_r)$, R_s and X_s are the equivalent resistance and reactance of the stator, respectively. R_r and X_r are the equivalent resistance and reactance of the rotor,

respectively. Other parameters can be calculated according to the following formula,

$$A=\left[\frac{M}{V_s}\quad\frac{1}{V_s}\quad 0\quad -\frac{u}{NX_mV_s}\right]^T,$$

$$B=\left[\frac{P_{sr}}{V_s}\quad 0\quad -\frac{X_sP_{sr}}{V_sX_m}\quad \frac{R_sP_{sr}}{V_sX_m}-\frac{V_s}{X_m}\right]^T,$$

where $P_{sr}=\frac{\omega_s}{\omega_r}P_{mec}$, $M=\frac{R_s}{X_s}$, and $N=\frac{X_s^2}{R_s^2+X_s^2}$.

3 Distributed voltage optimization control scheme

The distributed voltage optimization control scheme is realized based on ADMM and partitioning. The interactive information only includes the state of the coupling branch, which reduces the demand for data transmission. A parallel computing architecture can be adopted, and when the number of nodes increases, it has good scalability.

3.1 Concept of ADMM-based optimization method

The ADMM is an algorithm that is intended to blend the dual ascent decomposability with the superior convergence properties of the method of multipliers [15]. The algorithm solves problems in the form:

$$\begin{aligned}&\min\ f(x)+g(z)\\&s.t.\ Ax+Bz=c\end{aligned}\tag{15}$$

with variables $x\in\Re^n$ and $z\in\Re^m$, where $A\in\Re^{p\times n}$, $B\in\Re^{p\times m}$, and $c\in\Re^p$. f, and g are convex.

As in the method of multipliers, the augmented Lagrangian is formed as follows:

$$\begin{aligned}L_p(x,z,y)=&\ f(x)+g(z)+y^T(Ax+Bz-c)\\&+\frac{\rho}{2}\left\|Ax+Bz-c\right\|^2\end{aligned}\tag{16}$$

ADMM consists of the iterations,

$$\begin{aligned}x^{k+1}&:=\arg\min_x L_\rho(x,z^k,y^k)\\z^{k+1}&:=\arg\min_z L_\rho(x^{k+1},z,y^k)\\y^{k+1}&:=y^k+\rho(Ax^{k+1}+Bz^{k+1}-c)\end{aligned}\tag{17}$$

3.2 Concept of radial network partition

According to the optimization theory, the local optimal solution of a convex optimization problem is equal to the global optimal solution [27], which makes it possible to find the global optimal solution by using a partitioned distributed algorithm to solve the optimization problem. In the voltage control field, partitions are usually decided by the system operators themselves. How to partition efficiently or achieve better performance is not the key issue to be discussed in this paper.

For a distribution network or wind farm with a radial form, $G=(N, E)$ is represented as a radial network, where N is the set of network nodes, and E is the set of network lines. $e_{i,j}\in E$ represents a network branch, where $i, j\in N$. For the problem considered in this study, it is assumed that the distribution network and the wind farm are divided into n_{area} regions, respectively. The node set in the ith partition is represented as N_i, and the branch set in the ith partition is represented as E_i, where $i=\{1,2,\cdots,n_{area}\}$. The set of branches in the coupling region is denoised to $X_{i,j}$, where $i, j=\{1,2,\cdots,n_{area}\}$ and $i\neq j$. For example, as Fig. 4 shows,

$N_1=\{1,2,3,9\}$,

$N_2=\{3,4,5,6,9,10,11\}$,

$N_3=\{6,7,8,11,12\}$,

$X_{1,2}=\{e_{3,9}\}$, and $X_{2,3}=\{e_{10,11}\}$.

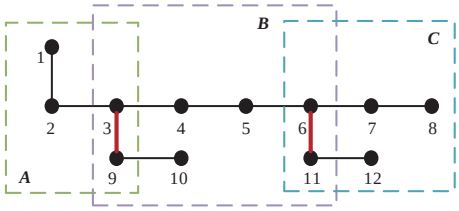

Fig. 4 Example of a radial network partition

3.3 ADMM-based grid optimization scheme

To make the partition problem equivalent to the original problem, the state variables of the coupling branch in each adjacent region must be equal. Therefore, the grid optimization objective can be decomposed into the distributed coordination calculation of sub-optimization problems in each region. The distributed reactive power optimization control model based on partition coordination is as follows:

$$\min\sum_{i=1}^{n_{area}}f_i(x_{grid,i})=\sum_{i=1}^{n_{area}}P_{grid,i}^{loss}\tag{18}$$

where i represents the ith partition in the network, $i, j=\{1,2,\cdots,n_{area}\}$. $x_{grid,i}$ represents the set of all state variables in the ith region, $x_{grid,i}=\{P_{i,mn},Q_{i,mn},U_{i,m},Q_{i,m}^{WF}\}$, where m and n represent the number of grid nodes, $m, n\in N_i$. $P_{i,mn}$ and $Q_{i,mn}$ are the active and reactive power from node m to node j in the ith region, respectively. $U_{i,m}$ is the voltage of node m, and $Q_{i,m}^{WF}$ is the reactive power produced by the WF connected to node m.

The constraints of this optimization problem are primarily considered from the power flow constraints, the safe operating condition of the power grid, the reactive power capacity constraints of the WFs, and ADMM

algorithm coupling constraints. That is, the constraints with the consideration of area partition are as follows:

$$P_{i,mn} = \sum P_{nk} - \frac{P_{i,mn}^2 + Q_{i,mn}^2}{V_{i,m}^2} R_{i,mn} - P_{i,n}^{load} + P_{i,n}^{WF} \quad (19)$$

$$Q_{i,mn} = \sum Q_{nk} - \frac{P_{i,mn}^2 + Q_{i,mn}^2}{V_{i,m}^2} X_{i,mn} - Q_{i,n}^{load} + Q_{i,n}^{WF} \quad (20)$$

$$V_{i,n}^2 = V_{i,m}^2 - 2(R_{i,mn}P_{i,mn} + X_{i,mn}Q_{i,mn}) + (R_{i,mn}^2 + X_{i,mn}^2)\frac{P_{i,mn}^2 + Q_{i,mn}^2}{V_{i,m}^2} \quad (21)$$

$$V_{1,1} = V_N \quad (22)$$

$$0.95\,p.u. \leqslant V_{i,m} \leqslant 1.05\,p.u. \quad (23)$$

$$\left|Q_{i,m}^{WF}\right| \leqslant Q_{i,m}^{WF\ \max} = \sqrt{\left(S_{i,m}^{WF}\right)^2 - \left(P_{i,m}^{WF}\right)^2} \quad (24)$$

$$X_i = X_j \quad (25)$$

where i is the ith region in the grid, $i = \{1, 2, \cdots, n_{area}\}$, and m, n, and k are the mth, nth, and kth nodes in the grid, respectively; $m, n, k = \{1, 2, \cdots, N\}$. The optimization problem of the entire system is decomposed into a coordinated calculation of sub-optimization problems of n_{area} regions.

To solve the above optimization problem by the ADMM method, the sub-objective function can be transformed into the sub-augmented Lagrangian function as shown below,

$$L_{grid,i} = P_{grid,i}^{loss} + \frac{\rho_{grid}}{2}\left\|x_{grid,i} - y_{grid,i} + \lambda_{grid,i}\right\|_2^2 \quad (26)$$

where ρ_{grid} is the penalty parameter of ADMM algorithm, and $y_{grid,i}$ is the global variable of the sub-optimization problem, where $y_{grid,i} = (x_{grid,i} + x_{grid,j})/2$. $\lambda_{grid,i}$ is a set of state variables in $X_{i,j}$, where $\lambda_{grid,i}(t+1) = \lambda_{grid,i}(t) + (x_{grid,i} - y_{grid,i})$.

Such that the optimization problem is defined as,

$$\min \sum_{i=1}^{n_{area}} L_{grid,i} \quad (27)$$

with the constraints of (19)–(25).

The specific procedure of the proposed algorithm is illustrated in Table 1.

Table 1 Procedure of ADMM-based optimization algorithm of the grid

Step 1	**Initialization:** divide the grid into n_{area} regions
Step 2	**Optimization:** solve the optimization problem in each region
Step 3	**Communication:** exchange coupling information with adjacent regions
Step 4	**Update:** calculate the global variable $y_{grid,i}$ and dual variable $\lambda_{grid,i}$
Step 5	**Evaluation:** determine whether it is satisfied with the convergence condition $y_{grid,i}(t+1) - y_{grid,i}(t) \leqslant \varepsilon$. If yes, output $Q_{i,m}^{WF}$ as the reactive power dispatch command for each WF; otherwise, go to Step 2.

3.4 ADMM-based optimization scheme of the WF

Similar to the grid optimization problem, the WF optimization problem can also be decomposed into distributed coordination calculation of sub-optimization problems in each region. The distributed reactive power optimization control model based on partition coordination is as follows:

$$\min \sum_{i=1}^{n_{feeder}} f_i(x_{WF,i}) = \sum_{i=1}^{n_{feeder}} (P_{WF,i}^{loss} - \sum_{j=1}^{n_{WT}} \omega_{i,j} Q_{i,j}) \quad (28)$$

where i is the ith region, $i, j = \{1, 2, \cdots, n_{areaWF}\}$, and $x_{WF,i}$ is the set of all state variables in the ith region; $x_{WF,i} = \{Q_{g,i,j}, U_{i,j}\}$, where j is the jth WT in the ith region. $P_{WF,i}^{loss}$ is the total loss of WTs and feeders in the ith region, where $P_{WF}^{loss} = P_{col}^{loss} + \sum_{i=1}^{n_{fd}} P_{fd}^{loss} + \sum_{i=1}^{n_{fd}} \sum_{j=1}^{n_{WT}} P_{WT,i,j}^{loss}$.

Owing to the existence of the wake effect [34], the WTs in the front receive more wind energy and produce more active power, thus having less reactive power potential. Similarly, the back WTs have greater reactive power potential. Therefore, $\omega_{i,j}$ is used to describe the output under the wake effect, where $\omega_{i,j}$ is represented as the weight of reactive power output of the jth WT in the ith region. It is supposed that the active power output of the WT is greater because the weight of the WT is less.

Constraints of the optimization problem are chiefly considered from power flow, reactive power capacity, and ADMM algorithm coupling constraints, that is, the constraints are as follows:

$$P_{i,j} = \sum P_{j,k} - P_j^{WT} \quad (29)$$

$$Q_{i,j} = \sum Q_{j,k} - Q_j^{WT} \quad (30)$$

$$V_{col}^2 = V_{slack}^2 - 2(R_{slack}P_{slack} + X_{slack}Q_{slack}) \quad (31)$$

$$V_{i,1}^2 = V_{col}^2 - 2(R_{fd,i}P_{fd,i} + X_{fd,i}Q_{fd,i}) \quad (32)$$

$$V_{i,j+1}^2 = V_{i,j}^2 - 2(R_{i,j}P_{i,j} + X_{i,j}Q_{i,j}) \quad (33)$$

$$Q_{slack} = Q_{WF}^{ref} \quad (34)$$

$$0.95\ p.u. \leqslant V_{i,j} \leqslant 1.05\ p.u. \quad (35)$$

To solve the above optimization problem by the ADMM method, the sub-objective function can be transformed into the sub-augmented Lagrangian function as shown below,

$$L_{WF,i} = P_{WF,i}^{loss} - \sum_{j=1}^{n_{WT}} \omega_{i,j} Q_{i,j} + \frac{\rho_{WF}}{2}\left\|x_{WF,i} - y_{WF,i} + \lambda_{WF,i}\right\|_2^2 \quad (36)$$

The definition of ρ_{WF}, $y_{WF,i}$, and $\lambda_{WF,i}$ is similar to the definition of the grid optimization problem.

Such that the optimization problem can be transformed into,

$$\min \sum_{i=1}^{n_{feeder}} L_{WF,i} \tag{37}$$

and the constraints are as (29)–(35) show.

The specific procedure of the proposed algorithm is illustrated in Table 2.

Table 2 Procedure of ADMM-based optimization algorithm of the WF

Step 1	**Initialization:** divide the WF into n_{areaWF} regions
Step 2	**Optimization:** solve the optimization problem in each region
Step 3	**Communication:** exchange coupling information with adjacent regions
Step 4	**Update:** calculate the global variable $y_{WF,i}$ and dual variable $\lambda_{WF,i}$
Step 5	**Evaluation:** determine whether it is satisfied with the convergence condition $y_{WF,i}(t+1)-y_{WF,i}(t)\leqslant\varepsilon$. If yes, output Q_j^{WT} as the reactive power dispatch command for each WF; otherwise, go to Step 2.

4 Simulation results

4.1 Case study setup

A distribution network (IEEE 33 bus system) with five WFs, with each WF having two feeders and 2 × 2 MW DFIG-based WTs connected to each feeder is used for validating the performance of the proposed strategies. The parameters of the DFIG-based WF can be found in [17], and the other parameters that are used in simulations are listed in Table 3.

Table 3 Parameters used in the simulation

Parameters	Value
Rated WF Power	8 MVA
Grid rated voltage	10 kV
Number of WTs on a Feeder	2
Number of Feeders in a WF	4
Nodes connected with a WF	7, 11, 15, 20, 25

4.2 Control strategies

Because the consensus ADMM algorithm is one of the key optimization methods based on ADMM adopted among recent articles, this paper primarily adopts three control strategies to conduct comparative simulations, as shown in the table below. Strategy A is the proposed two-stage optimization algorithm, and Strategies B and C are consensus control of the grid and WFs, respectively, which are dispatched with the reactive power commands according to the consensus protocol of the utilization ratio among the WFs in the grid and WTs in the WF, respectively.

Table 4 Control strategies adopted for comparison

Strategies	Description
Strategy A	The proposed two-stage optimization algorithm
Strategy B	Consensus control of the grid [22]
Strategy C	Consensus control of the WFs

4.3 Simulation results

A) Control performance of the proposed method

Assume that the coupling region of the grid and the WFs are as shown in Figs. 5 and 6, respectively. Considering the reactive power scheduling command issued by the TSO to be 1.55 p.u., the reactive power output assigned to each WF is shown in Table 5, and the outputs of each WT in the WFs connected to each node are shown in Table 6.

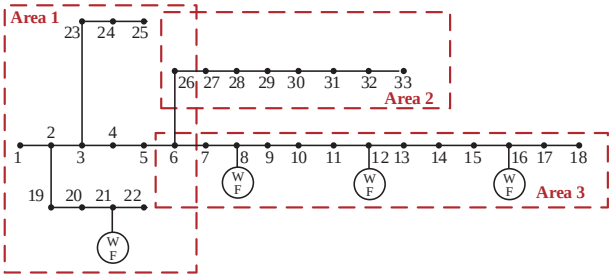

Fig. 5 Grid structure with partition

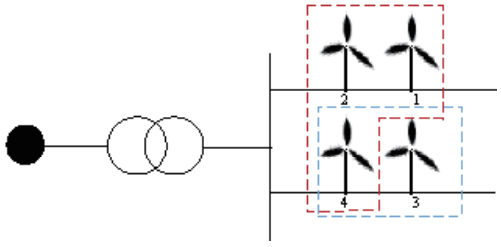

Fig. 6 WF structure with partition

Table 5 Reactive power output assigned to each WF

Node number	Reactive power output (p.u.)
7	0.04
11	0.18
15	0.15
20	0.13
25	1.05

Table 6 Reactive power output assigned to each WT in the WF

Node number	WT number	Reactive power output (p.u.)
7	1, 3	0
	2, 4	0.02
11	1, 3	0.0121
	2, 4	0.0779
15	1, 3	0.0046
	2, 4	0.0704
20	1, 3	0
	2, 4	0.065
25	1, 3	0.2296
	2, 4	0.2954

Distributed optimization is an iterative process. During each iteration, neighboring regions exchange coupling branch states. Communication times are positively correlated with optimization problem solving times. In the proposed algorithm, when the convergence conditions are set as $\varepsilon = 10^{-4}$, both grid and wind farm sides can achieve convergence within 70 iterations under a parallel computing structure, which meets the reactive power dispatch requirements.

B) Comparison with other strategies

As mentioned in Subsection 4.2, the comparative results are as shown in Table 7.

Table 7 Comparative results between four strategies

	Strategy	Total loss (p.u.)
Grid	A	0.0473
	B	0.0514
WF connected to node 7	A	0.0234
	C	0.0247
WF connected to node 11	A	0.0989
	C	0.1013
WF connected to node 15	A	0.0820
	C	0.0844
WF connected to node 20	A	0.0709
	C	0.0733
WF connected to node 25	A	0.6944
	C	0.6968

As observed from the above results, compared with the consensus ADMM based optimization, the total loss of the proposed optimization method is smaller under the same objective function. Thus, the effectiveness of the proposed method is verified.

5 Conclusions and discussions

Herein, we proposed a two-stage distributed reactive power output optimization control method considering wake effects for WFs and demonstrated the effectiveness and rationality of the proposed strategies. With the proposed method, each area only exchanges information of the coupled region with its neighbors, which effectively protects information privacy. The proposed optimization framework simultaneously achieves the goals of tracking TSO control commands, optimizing reactive power output of WFs at the distribution network level, and optimizing fan output at the WF level. The performance and convergence of the proposed method were verified via simulations considering the IEEE 33-bus and 4 × 2 MW WF systems.

However, this study only discussed the response of the distribution network and WF sides to the TSO dispatching commands. The dynamic response of the proposed method under variable wind speed conditions and the autonomous response under voltage fluctuation conditions should be considered in future studies.

Acknowledgements

The authors would like to thank the support of The National Key Research and Development Program of China (Basic Research Class) (No. 2017YFB0903000), and the National Natural Science Foundation of China (No. U1909201).

Declaration of Competing Interest

We declare that we have no conflict of interest.

References

[1] Guo Y F, Gao H L, Wu Q W (2019) Distributed cooperative voltage control of wind farms based on consensus protocol. International Journal of Electrical Power & Energy Systems, 104: 593-602

[2] Martínez J, Kjær P C, Rodriguez P et al (2011) Comparison of two voltage control strategies for a wind power plant. 2011 IEEE/PES Power Systems Conference and Exposition. Phoenix, AZ, USA. IEEE, 1-9

[3] Tapia G, Tapia A, Ostolaza J X (2007) Proportional–integral regulator-based approach to wind farm reactive power management for secondary voltage control. IEEE Transactions on Energy Conversion, 22(2): 488-498

[4] Ko H S, Bruey S, Jatskevich J et al (2007) A PI control of DFIG-based wind farm for voltage regulation at remote location. 2007 IEEE Power Engineering Society General Meeting, 1-6

[5] Neumann T, Erlich I, Paz B et al (2016) Novel direct voltage control by wind turbines. 2016 IEEE Power and Energy Society General Meeting (PESGM), 1-5

[6] Chi Y, Xu Y, Zhang R (2021) Many-objective robust optimization for dynamic VAR planning to enhance voltage stability of a wind-energy power system. IEEE Transactions on Power Delivery, 36(1): 30-42

[7] Zhao J J, Li X, Hao J T et al (2009) Wind farm reactive power output optimization for loss reduction and voltage profile improvements. 2009 IEEE 6th International Power Electronics and Motion Control Conference. Wuhan, China. IEEE, 1099-1103

[8] He Y F, Wang M H, Xu Z (2020) Coordinative low-voltage-ride-through control for the wind-photovoltaic hybrid generation system. IEEE Journal of Emerging and Selected Topics in Power Electronics, 8(2): 1503-1514

[9] Chen M L N, Jiang L J, Sha W (2017) Ultrathin complementary metasurface for orbital angular momentum generation at microwave frequencies. IEEE Transactions on Antennas and Propagation, 65(1): 396-400

[10] Chen M L N, Jiang L J, Lan Z H et al (2020) Coexistence of pseudospin- and valley-Hall-like edge states in a photonic crystal with C3v symmetry. Physical Review Research, 2(4): 043148

[11] Wang M H, Yan S, Tan S C et al (2020) Decentralized control of DC electric springs for storage reduction in DC microgrids. IEEE Transactions on Power Electronics, 35(5): 4634-4646

[12] Teixeira Pinto R, Bauer P, Rodrigues S F et al (2013) A novel distributed direct-voltage control strategy for grid integration of offshore wind energy systems through MTDC network. IEEE Transactions on Industrial Electronics, 60(6): 2429-2441

[13] Farag H E Z, El-Saadany E F (2013) A novel cooperative protocol for distributed voltage control in active distribution systems. IEEE Transactions on Power Systems, 28(2): 1645-1656

[14] Anilkumar R, Devriese G, Srivastava A K (2018) Voltage and reactive power control to maximize the energy savings in power distribution system with wind energy . IEEE Transactions on Industry Applications, 54(1): 656-664

[15] Boyd S Distributed optimization and statistical learning via the alternating direction method of multipliers. Now Publishers Inc, 2010

[16] Guo Y F, Gao H L, Xing H et al (2019) Decentralized coordinated voltage control for VSC-HVDC connected wind farms based on ADMM. IEEE Transactions on Sustainable Energy, 10(2): 800-810

[17] Huang S, Li P Y, Wu Q W et al (2020) ADMM-based distributed optimal reactive power control for loss minimization of DFIG-based wind farms. International Journal of Electrical Power & Energy Systems, 118: 105827

[18] Wei S R, Zhang L, Xu Y et al (2017) Hierarchical optimization for the double-sided ring structure of the collector system planning of large offshore wind farms. IEEE Transactions on Sustainable Energy, 8(3): 1029-1039

[19] Kim J, Muljadi E, Park J W et al (2016) Adaptive hierarchical voltage control of a DFIG-based wind power plant for a grid fault. IEEE Transactions on Smart Grid, 7(6): 2980-2990

[20] Kong X B, Liu X J, Ma L L et al (2019) Hierarchical distributed model predictive control of standalone wind/solar/battery power system. IEEE Transactions on Systems, Man, and Cybernetics: Systems, 49(8): 1570-1581

[21] Tavakoli M, Shokridehaki F, Marzband M et al (2018) A two stage hierarchical control approach for the optimal energy management in commercial building microgrids based on local wind power and PEVs. Sustainable Cities and Society, 41: 332-340

[22] Huang S, Wu Q W, Guo Y F et al (2020) Distributed voltage control based on ADMM for large-scale wind farm cluster connected to VSC-HVDC. IEEE Transactions on Sustainable Energy, 11(2): 584-594

[23] Liao W, Li P Y, Wu Q W et al (2021) Distributed optimal active and reactive power control for wind farms based on ADMM. International Journal of Electrical Power & Energy Systems, 129: 106799

[24] Huang S, Gong Y S, Wu Q W et al (2020) Two-tier combined active and reactive power controls for VSC–HVDC-connected large-scale wind farm cluster based on ADMM. IET Renewable Power Generation, 14(8): 1379-1386

[25] Abessi A, Vahidinasab V, Ghazizadeh M S (2016) Centralized support distributed voltage control by using end-users as reactive power support. IEEE Transactions on Smart Grid, 7(1): 178-188

[26] Xu T, Wu W C (2020) Accelerated ADMM-based fully distributed inverter-based volt/var control strategy for active distribution networks. IEEE Transactions on Industrial Informatics, 16(12): 7532-7543

[27] Tian, J., Zhou, D., Su, C., Chen, Z., & Blaabjerg, F. (2016). Reactive power dispatch method in wind farms to improve the lifetime of power converter considering wake effect. IEEE Transactions on Sustainable Energy, 8(2), 477-487

[28] Tian J, Zhou D, Su C et al (2017) Reactive power dispatch method in wind farms to improve the lifetime of power converter considering wake effect. IEEE Transactions on Sustainable Energy, 8(2): 477-487

[29] Lyu X, Jia Y W, Xu Z (2020) A novel control strategy for wind farm active power regulation considering wake interaction. IEEE Transactions on Sustainable Energy, 11(2): 618-628

[30] Shakoor R, Hassan M Y, Raheem A et al (2016) Wake effect modeling: A review of wind farm layout optimization using Jensen′s model. Renewable and Sustainable Energy Reviews, 58: 1048-1059

[31] Tian J, Zhou D, Su C et al (2017) Wind turbine power curve design for optimal power generation in wind farms considering wake effect. Energies, 10(3): 395

[32] Yang K, Kwak G, Cho K et al (2019) Wind farm layout optimization for wake effect uniformity. Energy, 183: 983-995

[33] Abad G, López J, Rodríguez M A et al (2011) Doubly fed induction machine. Hoboken, NJ, USA: John Wiley & Sons, Inc.

[34] Li Y J, Xu Z, Zhang J L et al (2018) Variable droop voltage control for wind farm. IEEE Transactions on Sustainable Energy, 9(1): 491-493

Biographies

Zhenming Li received her B.E.E degree at Zhejiang University, Hangzhou, China, in 2017. She is currently pursuing a Ph.D. degree with the College of Electrical Engineering, Zhejiang University, Hangzhou, China. Her current research interests include voltage optimization and control of renewable energy and cyber-physical security with application in smart grids.

Zhao Xu received the B.Eng., M. Eng., and Ph.D. degrees from Zhejiang University, Hangzhou, China, in 1996, National University of Singapore, Singapore, in 2002, and The University of Queensland, Brisbane, QLD, Australia, in 2006, respectively. He is currently a Professor with the Department of Electrical Engineering, Hong Kong Polytechnic University, Hong Kong. He was with the Centre for Electric Power and Energy, Technical University of Denmark. His research interests include demand side, grid integration of renewable energies and EVs, electricity market planning and management, and AI applications in power engineering. He is an Editor for the IEEE Transactions on Smart Grid, the IEEE Power Engineering Letters, and Electric Power Components and Systems journal.

Yawen Xie received her Bachelor degree in electrical engineering and automation from North China Electric Power University, BaoDing, China, in 2011.Now she works in Quzhou Power Supply Company, Zhejiang Electric Power Company of State Grid, and is engaged in electrical design and automation of distribution power system.

Donglian Qi received the Ph.D. degree in control theory and control engineering from Zhejiang University, Hangzhou, China, in March 2002. Since then, she has been with the College of Electrical Engineering, Zhejiang University where she is currently a Professor. Her current research interests include the basic theory and application of cyber physical power system (CPPS), digital image processing, artificial intelligence, and electric operation and maintenance robots. She is an Editor for the Clean Energy, the IET Energy Conversion and Economics, and the Journal of Robotics, Networking and Artificial Life.

Jianliang Zhang received his Ph.D. degree in control theory and control engineering from Zhejiang University, Hangzhou, China, in June 2014. Since then, he has been working with the College of Electrical Engineering, Zhejiang University (ZJU). He was a visiting scholar at Hongkong Polytechnic University (PolyU) (2016-2017). His current research interests include distributed optimization, with applications to energy/power systems, and cyber-physical security with application in smart grids.

(Editor Yanbo Wang)